

Origin of the 1.54 μm luminescence of erbium-implanted porous silicon

Jung H. Shin, G. N. van den Hoven, and A. Polman

FOM Institute for Atomic and Molecular Physics, Kruislaan 407, 1098 SJ Amsterdam, The Netherlands

(Received 21 November 1994; accepted for publication 1 March 1995)

Photoluminescence of erbium-implanted porous silicon is investigated. Room temperature 1.54 μm Er^{3+} luminescence is observed after annealing. The luminescence spectrum, annealing characteristics, temperature quenching, and the luminescence lifetime suggest that the Er^{3+} luminescence is mediated by photocarriers in the amorphous silicon matrix in porous silicon, and not related to the presence of the crystal nanograins. © 1995 American Institute of Physics.

Er^{3+} is a rare earth ion that can undergo an optical transition near 1.54 μm . As this wavelength coincides with the low-loss window in silica-based optical fibers, a tremendous amount of research activity has been devoted to the study of Er-doped materials for potential use in optoelectronic components.¹ In particular, Er-doped silicon is under intensive investigation as a possible silicon-based light source, circumventing the inefficiency of silicon in generating light due to its indirect band gap, and offering compatibility with the vast silicon-based integrated circuit technology.² Recently, room temperature electroluminescence of Er-doped silicon-based devices has been reported.³⁻⁵

Interest is now also being focused on Er-doped porous silicon. Porous silicon (*p*-Si) luminesces brightly in the visible range, generally thought to be due to quantum confinement of carriers in silicon crystal nanograins present in *p*-Si.⁶ Erbium has been incorporated in *p*-Si either through ion implantation⁷ or through electrolysis.⁸ In both cases, room temperature photoluminescence of Er was reported. Excitation of Er^{3+} in crystalline Si is known to occur through carrier recombination and subsequent energy transfer to Er^{3+} ions.⁹ It was suggested that in *p*-Si, spatial confinement of photocarriers in silicon nanograins would cause them to recombine near the incorporated Er, thus resulting in very efficient excitation of Er^{3+} .^{7,8}

However, direct evidence for this model is still lacking. Furthermore, *p*-Si is a disordered system, containing not only crystal nanograins but also amorphous regions and high concentrations of oxygen and hydrogen.^{10,11} Erbium incorporated into such an amorphous mixture of silicon, oxygen, and hydrogen (hereafter referred to as *a*-Si:O:H, but also known as SIPOS) has been shown to luminesce efficiently at room temperature.^{12,13} In this paper, we will present results that show that the observed Er luminescence in *p*-Si is indeed due to Er^{3+} ions incorporated into such an amorphous matrix, and not related to the presence of crystal nanograins.

A 5–10 μm thick layer of *p*-Si was produced by anodic etching of a silicon wafer in a 2:3:5 HF/H₂O/2-propanol solution for 10 min at a current density of 20 mA/cm². The resulting porosity is 65%. The Si to O ratio in the *p*-Si layer was 1:1 as analyzed by Rutherford backscattering spectroscopy, confirming the abundance of oxygen in *p*-Si. The *p*-Si film was implanted with Er at 250 keV to a dose of $1 \times 10^{15}/\text{cm}^2$ at room temperature, and annealed in vacuum (based pressure $\leq 1 \times 10^{-6}$ mbar) for 2 h at various temperatures. The projected range of 250 keV Er in a 1:1 Si/O

mixture corresponds to a layer of 5.5×10^{17} at./cm², i.e., 250 nm for a film of 65% porosity. For comparison, materials other than *p*-Si were also implanted with Er and annealed to obtain optimum Er^{3+} luminescence. These materials are as follows: an *a*-Si:O:H film containing 31 at. % O and 23 at. % H formed by low pressure chemical vapor deposition (fluence: 1×10^{15} Er/cm²; anneal: 400 °C for 30 min)¹³ Czochralski (CZ) grown Si (100) (fluence: 7×10^{14} Er/cm²; anneal: 600 °C for 15 min+1100 °C for 15 s),¹⁴ and thermally grown SiO₂ (fluence: 1.9×10^{15} Er/cm²; anneal: 900 °C for 30 min).¹⁵ Photoluminescence spectra were measured using an Ar laser as the excitation source, and employing a mechanical chopper and standard lock-in techniques. The pump power was in the 5–50 mW range. A photomultiplier tube was used for measurements in the visible range, while a liquid nitrogen cooled Ge detector was used for the infrared range. All spectra were corrected for detector sensitivities. A closed-cycle helium cryostat was used for low temperature measurements, and an averaging, digitizing oscilloscope was used for photoluminescence lifetime measurements.

Figure 1 shows the room temperature photoluminescence spectra of *p*-Si prior to implantation, after implantation, and after subsequent annealing at 400 °C. The pump intensity was 5 mW for the visible luminescence, and 50 mW for

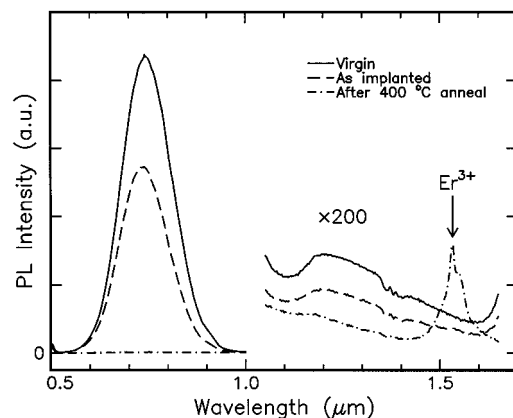


FIG. 1. Room temperature photoluminescence spectra of virgin, Er-implanted, and Er-implanted and annealed porous silicon. The excitation source was the 455 nm line of the Ar laser. The pump power was 5 mW for the visible luminescence, and 50 mW for the infrared ($\geq 1 \mu\text{m}$) luminescence. Note that the infrared luminescence has been scaled by a factor of 200.

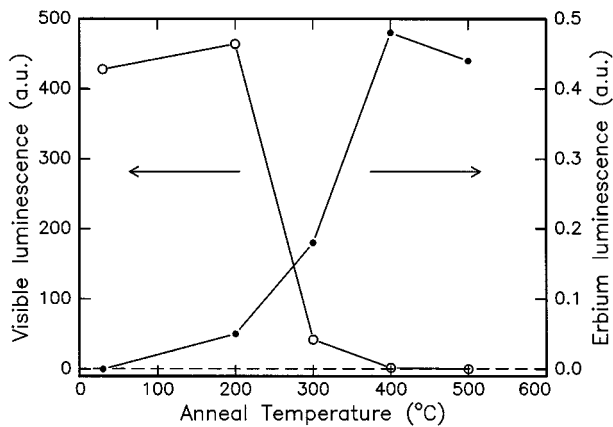


FIG. 2. Integrated visible and Er luminescence as a function of annealing temperature, measured at room temperature.

the infrared ($\geq 1\mu\text{m}$) luminescence. Prior to implantation, the visible luminescence from *p*-Si is quite intense and visible to the naked eye in ambient light, confirming the good quality of the *p*-Si layer. Even after irradiation, the visible luminescence peak is still intense, and nearly identical in shape to the luminescence peak prior to irradiation. Since ion irradiation is known to quench visible luminescence,¹⁶ we attribute the observed visible luminescence after implantation to the deeper part of the *p*-Si lying beyond the range of the implanted ions. No Er-related luminescence can be observed in the as-implanted sample, and anneals are necessary to obtain $1.54\mu\text{m}$ luminescence from Er^{3+} .

Figure 2 shows the integrated room temperature visible and Er^{3+} luminescence intensities as functions of annealing temperature. Maximum Er luminescence is obtained following an anneal at 400°C . Therefore, this sample was used in all following experiments. After such an anneal, however, the visible luminescence is reduced by nearly three orders of magnitude, and is in fact barely measurable. Such a decrease in visible luminescence intensity following annealing has been observed before, and was correlated with the loss of hydrogen.¹⁷ Hydrogen serves to passivate the large surface area of *p*-Si. Loss of hydrogen probably results in creation of defects that act as nonradiating recombination sites of carriers, thereby quenching the luminescence. Indeed, the luminescence lifetime of the visible luminescence was measured (not shown), and confirmed to decrease with increasing annealing temperature.

Figure 3 shows the temperature dependence of both visible and Er luminescence in *p*-Si. Again, the behavior of the visible luminescence, attributed to carrier recombination in the crystalline Si nanograins, and that of the Er luminescence are quite different. The visible luminescence is quenched by a factor of ~ 20 as the temperature is increased from 15 K to room temperature, indicating activation of nonradiative recombination centers for carriers. The Er^{3+} luminescence, on the other hand, decreases less than twofold.

If transfer of the energy from carrier recombination in the crystal nanograins to Er^{3+} were the excitation mechanism of Er^{3+} in *p*-Si, then as defect-related, nonradiative carrier recombination centers become dominant (as indicated by

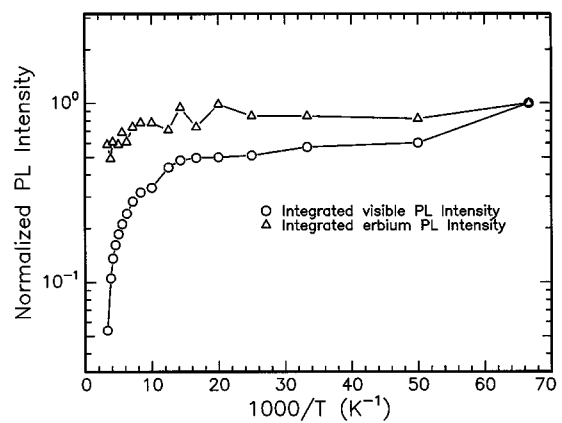


FIG. 3. Arrhenius plot of the temperature dependence of integrated visible and Er luminescence, for the sample annealed at 400°C .

quenching of the visible luminescence), the Er^{3+} luminescence should also be quenched. However, as Figs. 1–3 show, there is no correlation between visible luminescence and Er^{3+} luminescence. Taken together, the data suggest that the silicon crystal grains do not play a major role in the luminescence of Er^{3+} in *p*-Si.

The excitation mechanism of Er in *p*-Si was further investigated by measuring the $1.54\mu\text{m}$ Er^{3+} luminescence intensity as a function of pump wavelength, at a fixed pump power of 50 mW using an Ar laser. The absorption coefficient of pure Si is $\sim 0.5\mu\text{m}$ for the pump wavelengths investigated, and decreases monotonically with increasing wavelength. Figure 4 shows the measured excitation spectrum. Also shown for comparison is the luminescence intensity of Er-implanted SiO_2 . The Er luminescence in SiO_2 shows distinct peaks near the pump wavelengths of 515 and 488 nm, reflecting the structure of the optical absorption bands of Er^{3+} . In contrast, the Er^{3+} luminescence in *p*-Si shows no such structure, showing that excitation is photocarrier mediated, and not mediated through direct optical absorption.

To further examine the local environment of Er in *p*-Si, photoluminescence spectra of Er-implanted crystalline

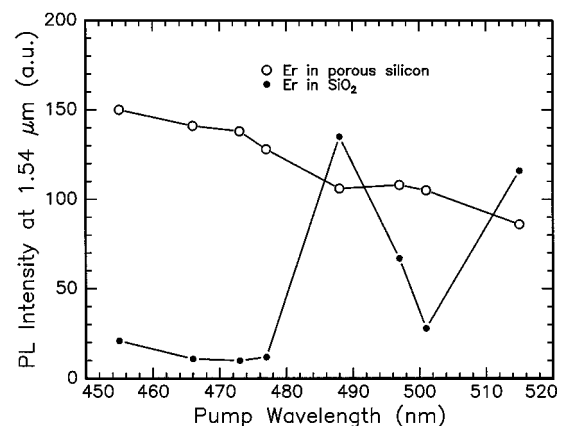


FIG. 4. Photoluminescence excitation spectra of Er-implanted and annealed porous silicon ($1 \times 10^{15} \text{Er}/\text{cm}^2 + 400^\circ\text{C}$) and SiO_2 ($1.9 \times 10^{15} \text{Er}/\text{cm}^2 + 900^\circ\text{C}$). Shown is the Er intensity at $1.54\mu\text{m}$, measured at room temperature at a constant pump power of 50 mW.

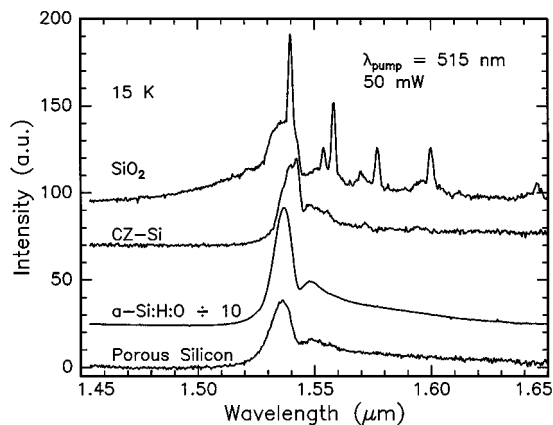


FIG. 5. Photoluminescence spectra of Er-implanted and annealed porous silicon (1×10^{15} Er/cm 2 + 400 °C), *a*-Si:O:H (1×10^{15} Er/cm 2 + 400 °C), CZ-Si (7×10^{14} Er/cm 2 + 600 °C + 1100 °C), and SiO $_2$ (1.9×10^{15} Er/cm 2 + 900 °C). Curves are offset for clarity. The signal from *a*-Si:O:H is divided by a factor of 10.

silicon, SiO $_2$, *a*-Si:O:H, and *p*-Si were measured at 15 K, all under identical measurement conditions. Figure 5 shows the results. The spectrum of Er in *p*-Si, with its two broad peaks without any sharp features, is very much unlike that of Er in crystalline silicon or in SiO $_2$. However, it is nearly identical to that of Er in *a*-Si:O:H, suggesting that Er $^{3+}$ ions in *p*-Si are in an environment similar to *a*-Si:O:H. Indeed, the dependence of Er luminescence intensity in *p*-Si on the annealing temperature (Fig. 2) and the temperature quenching of luminescence (Fig. 3) are nearly identical to that of Er in *a*-Si:O:H.¹³ The luminescent decay of Er in *p*-Si was also measured (not shown), and found to be very similar to that of Er in *a*-Si:O:H, further supporting the argument that Er in *p*-Si is incorporated into an environment similar to *a*-Si:O:H. Changes in the oxygen and hydrogen content of the material will therefore influence the photoluminescence of Er much more strongly than changes in porosity or crystal nanograin size, which on their own have no effect on the Er-luminescence.

In conclusion, we have measured the photoluminescence of Er-implanted *p*-Si. Although we can corroborate previous findings of 1.54 μm Er $^{3+}$ luminescence, we find evidence

that the presence of Si crystal nanograins in *p*-Si is not essential for the observed Er luminescence, contrary to earlier claims.^{7,8} Rather, we find strong similarities between Er luminescence in *p*-Si and in *a*-Si:O:H, suggesting that the observed Er luminescence in *p*-Si is due to Er atoms incorporated into such amorphous regions in *p*-Si.

We would like to thank A. H. J. Venhuizen, Y. A. R. R. Kessener, and H. van Houten from Philips Research Labs (Eindhoven) for fabricating and providing the *p*-Si, and S. Lombardo from the University of Catania (Italy) for providing the *a*-Si:O:H samples. This work is part of the research program of the Foundation for Fundamental Research on Matter (FOM), and was made possible by financial support from the Dutch Organization for the Advancement of Research (NWO), the Foundation for Technical Research (STW), and the IC Technology Program (IOP Electro-Optics) of the Ministry of Economic Affairs.

¹ See, for example, Mater. Res. Soc. Symp. Proc. **301** (1993).

² H. Ennen, J. Schneider, G. Pomrenke, and A. Axmann, Appl. Phys. Lett. **43**, 943 (1983).

³ G. Franzò, F. Priolo, S. Coffa, A. Polman, and A. Carnera, Appl. Phys. Lett. **64**, 2235 (1993).

⁴ B. Zhen, J. Michel, F. Y. G. Ren, L. C. Kimerling, D. C. Jacobson, and J. M. Poate, Appl. Phys. Lett. **64**, 2842 (1994).

⁵ S. Lombardo, S. U. Campisano, G. N. van den Hoven, and A. Polman, J. Appl. Phys. (to be published).

⁶ L. T. Canham, Appl. Phys. Lett. **57**, 1046 (1990).

⁷ F. Namavar, III-V Rev. **7**, 10 (1994), and presented at Rare Earth Doped Optoelectronic Materials Workshop, Malibu, CA, June 16, 1994.

⁸ T. Kimura, A. Yokoi, H. Horiguchi, R. Saito, T. Ikoma, and A. Sato, Appl. Phys. Lett. **65**, 983 (1994).

⁹ A. Polman, G. N. van den Hoven, J. S. Custer, J. H. Shin, R. Serna, and P. F. A. Alkemade, J. Appl. Phys. **77**, 1256 (1995).

¹⁰ I. Berbezier and A. Halimaoui, J. Appl. Phys. **74**, 5421 (1993).

¹¹ J. M. Perez, J. Villalobos, P. McNeil, J. Prasad, R. Cheek, J. Kelber, J. P. Esterera, P. D. Stevens, and R. Glosser, Appl. Phys. Lett. **61**, 563 (1992).

¹² S. Lombardo, S. U. Campisano, G. N. van den Hoven, A. Cacciato, and A. Polman, Appl. Phys. Lett. **63**, 1942 (1993).

¹³ G. N. van den Hoven, J. H. Shin, A. Polman, S. Lombardo, and S. U. Campisano (unpublished).

¹⁴ A. Polman, J. S. Custer, E. Snoeks, and G. N. van den Hoven, Nucl. Instrum. Methods B **80/81**, 653 (1993).

¹⁵ A. Polman, D. C. Jacobson, D. J. Eaglesham, R. C. Kistler, and J. M. Poate, J. Appl. Phys. **70**, 3778 (1991).

¹⁶ J. C. Barbour, D. Dimos, T. R. Guilinger, M. J. Kelly, and S. S. Tsao, Appl. Phys. Lett. **59**, 2088 (1991).

¹⁷ C. Tsai, K. H. Li, J. Sarathy, S. Shih, J. C. Campbell, B. K. Hance, and J. M. White, Appl. Phys. Lett. **59**, 2814 (1991).